Adsorption (2024) 30:783–800
https://doi.org/10.1007/s10450-024-00461-y

Performance and optimization of diclofenac and ibuprofen adsorption onto activated carbon synthesized from sunflower seed shell (Helianthus annuus) in natural groundwater samples

John J. Alvear-Daza[1] · Julián A. Rengifo-Herrera[1] · Luis René Pizzio[1]

Received: 6 March 2024 / Revised: 20 March 2024 / Accepted: 21 March 2024 / Published online: 14 April 2024

Abstract

In this study, activated carbon (AC) obtained from biomass waste materials (sunflower seed shells -SSS) was synthesized by combining chemical (H_3PO_4 80% wt.) and thermal activation (at 544 °C). Synthesized AC exhibited a BET surface area of 1531 $m^2\ g^{-1}$, and pore volume of 0.98 $cm^3\ g^{-1}$. The material exhibited various surface functional groups, such as P_2O_7, C-O-P and -COOH, O = C, as well as a moderate graphitization degree ($I_D/I_G < 1$) and acidity caused by H_3PO_4 treatment. Moreover, its morphology and physicochemical features were evaluated by SEM–EDS, TGA, XPS, Raman, and FT-IR techniques. The material was used to study the adsorption of anti-inflammatory pharmaceutical compounds such as ibuprofen (IBF) and diclofenac (DIF) present in natural groundwater samples. The effects of parameters such as pH, activated carbon dose, temperature, and IBF or DIF initial concentration were optimized by using a central composite design (CCD). The results revealed that optimum conditions to remove DIF and IBF from natural groundwater samples were pH of 8.0 and 7.0, an AC dose of 0.79 and 1.0 g L^{-1}, and a contact time of 60 min for DIF and IBF, respectively. A successful procedure to desorb both pollutants from adsorbent by using acetonitrile solutions was achieved, allowing the reuse study whose main results were that after four reusing cycles AC reduced its efficiency to remove DIF and IBF in 28 and 34%, respectively. Finally, the effect of ions, such as nitrate, bicarbonate, and sulfate at concentrations commonly found in natural groundwater on the adsorption of both pollutants onto AC was studied using deionized water. As a result, this study suggests considerable interest of AC in real applications due to its versatility and prolonged reuse to effectively remove anti-inflammatory compounds from natural aqueous solution.

✉ Julián A. Rengifo-Herrera
julianregifo@quimica.unlp.edu.ar

✉ Luis René Pizzio
lrpizzio@quimica.unlp.edu.ar

[1] Laboratory of Advanced Oxidation Processes and Photocatalysis (LAPh), Centro de Investigación y Desarrollo en Ciencias Aplicadas “Dr. J.J. Ronco” (CINDECA), Departamento de Química, Facultad de Ciencias Exactas, UNLP-CCT La Plata, CONICET, 47 No. 257, 1900 La Plata, Buenos Aires, Argentina

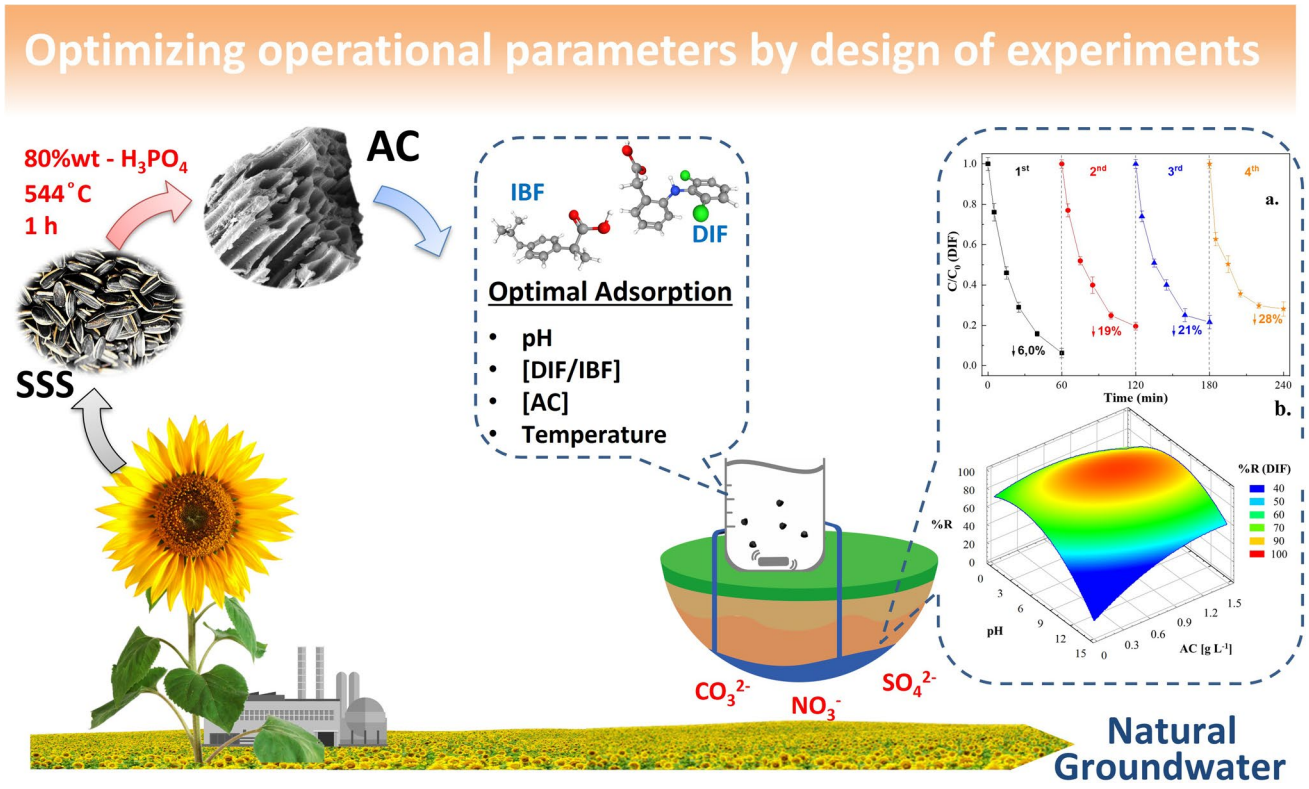

Highlights

- Optimal conditions for the pollutants adsorption were found by an experimental design
- Adsorption of pollutants on activated carbon was studied in groundwater samples
- Good adsorbent properties of activated carbon remained even after 4 reusing cycles
- Activated carbon exhibited several functional groups and high specific surface area
- The effect of ions present in groundwater on pollutants adsorption was studied

Keywords Activated carbon · CCD · Diclofenac · Groundwater · Ibuprofen · Sunflowers seed shell

1 Introduction

Due to their bioactive properties, pharmaceutical and personal care products (PPCPs) in the environment are considered contaminants of emerging concern (CECs) and have been frequently detected in soils and groundwater [11]. The primary sources of PCPPs in groundwater include domestic, hospital, and industrial effluents, animal wastes, landfill leachates, and rivers that may infiltrate groundwater through hydraulic exchange [24, 37]. In this context, the PCPPs found more frequently in natural waters around the world are carbamazepine, sulfamethoxazole, ibuprofen, and caffeine while diclofenac has been found in European groundwater samples [16].

Ibuprofen (IBF) and diclofenac (DIF) are members of non-steroidal anti-inflammatory drugs (NSAIDs) and constitute a group of pharmaceuticals with analgesic, antipyretic and inflammatory effects. However, IBF presents, slight solubility (21 mg L^{-1}), and high mobility in the water while DIF has high water solubility (5000 mg L^{-1}). Because DIF and IBF has an excessive consumption, they have been detected in natural water and wastewater resources around the world [1, 6]. In addition, it has been reported that only 62% and 18% are eliminated by conventional treatment systems in wastewater treatment plants (WWTP) for DI and IB [8, 20]. Therefore, different technologies such as oxidation processes [44, 46], electrochemical degradation [10], photo-degradation [44, 46], and membrane ultrafiltration [9, 45], have been explored to remove NSAIDs from water. Unfortunately, these technologies exhibit some drawbacks related to high operational costs, the generation of toxic

byproducts, and the possible leaching of chemicals. However, the adsorption processes using low-cost materials such as activated carbon or biochar from agro-industrial wastes seem to be promising for removing pharmaceuticals from water [32]. Carbonaceous materials such as activated carbon (AC) exhibit an amorphous arrangement of bonded carbon atoms that form a porous structure with pore sizes ranging from the molecular level to visible cracks and crevices. AC, pore structures, surface area, and surface chemistry vary with feedstock and activation conditions [32].

Several agro-industrial wastes such as olive stone, tea waste, rice husk, cocoa shell, cork powder, and peach stone have been used as precursors to synthesize carbonaceous materials and have been evaluated in the adsorption of pharmaceuticals dissolved in water. For instance, several papers reported diclofenac removal by carbonaceous adsorbents synthesized from tea wastes [25], cocoa shells [34], olive wastes [5], and peach stones [41] obtaining values of maximum adsorption capacity (Q_{max}) of 62 mg g^{-1}, 63.5 mg g^{-1}, 56.2 mg g^{-1}, and 200 mg g^{-1}, respectively. Regarding ibuprofen adsorption, it was found that AC synthesized from rice husk [2], cork powder [28], and agave sisalana [27] were able to remove it from water obtaining values of Q_{max} around 239.8 mg g^{-1}, 320 mg g^{-1}, 325 mg g^{-1}, respectively. Previous work reported by us [3] assessed to the optimal experimental conditions to synthesize activated carbon from sunflower seed shells (using H_3PO_4 as activating agent, at concentrations of 80% (wt./wt.), and a carbonizing temperature of 544 $^{\circ}$C). This material was evaluated in the removal of methylene blue, diclofenac, and ibuprofen obtaining Q_{max} adsorption values of 546, 692, and 105 mg g^{-1}, respectively. Activated carbon was deeply characterized through different techniques allowing to suggest the possible adsorption mechanisms. However, it is necessary to study the adsorption of both contaminants in natural water samples to optimize the experimental parameters for the removal of DIF and IBF in a complex aqueous matrix, and to study desorption and regeneration treatments to improve the recycling of ACs. The novelty of this work lies in the fact that, unlike other studies, we focus on evaluating the adsorption efficiency by using robust statistical methods using different initial concentrations of the contaminants added to real groundwater samples.

Herein, the optimal adsorption processes of DIF and IBF in synthetic and natural groundwater samples using activated carbon from sunflower seed shells (SSS) was studied. We evaluated the adsorption capacity of both pharmaceuticals considering key parameters such as initial pH solution, DIF or IBF initial concentration, AC dosage, and temperature. Furthermore, DIF and IBF adsorption process was optimized using a response surface methodology (RSM) of type central composite experimental design (CCD) – 2^3 in 3 blocks. Finally, the effect of ions typically found in natural groundwater samples, such as nitrate, carbonate species, and sulfate at environmental concentrations, on DIF and IBF adsorption was studied in deionized water.

2 Materials and methods

2.1 Chemicals

Phosphoric acid (H_3PO_4) 85% (Anedra®), sodium hydroxide (NaOH) 94% (Anedra®), hydrochloric acid (HCl) 37% (Anedra®), acetonitrile (CH_3CN) (PanReac-AppliChem), sodium sulfate (Na_2SO_4) 99% (Sigma-Aldrich), sodium nitrate ($NaNO_3$) 99% (Sigma-Aldrich), sodium bicarbonate ($NaHCO_3$) 99.7% (Sigma-Aldrich), diclofenac sodium (Parafarm-Saporiti), R/S-ibuprofen (Parafarm-Saporiti) with a purity of 99.3% and 99.5%, respectively.

2.2 Characterization of activated carbon adsorbent

Synthesis of AC was performed using a methodology previously reported by us [3]. Briefly, 100 g of sunflower seed shell (SSS) was washed with deionized water and dried at 100 °C for 12 h. The SSS samples were screened through the ASTM sieve size # 40—170 to produce particle sizes between 0.42 and 0.09 mm. Then, 10–20 g of SSS samples were treated with phosphoric acid (80%wt.) (as an activating agent) and heated at 75 °C, for 1 h with constant stirring at 350 rpm. Finally, The sample was carbonized at 544 °C for 1 h (5 °C min^{-1} heating rate) under nitrogen atmosphere using an oven Estigia ® (Argentina).

2.3 Characterization of activated carbon adsorbent

The characterization of the materials was performed by scanning electron microscopy (SEM Phillips 505) equipped with an X-ray energy dispersive analyzer (EDAX-9100). Textural properties were evaluated by N_2 adsorption–desorption at 77 K using an equipment (Micromeritics ASAP 2010).

For its part, Fourier-transform infrared spectroscopy (FT-IR) measurements were performed in a FT-IR spectrometer using Bruker IFS 66 equipment and spectra were recorded using 1024 scans having a resolution of 4 cm^{-1}. Raman spectra were collected using a Raman microspectrometer (Raman, Horiba Jobin Yvon T64000) with Ar laser at 514.5 nm. Thermogravimetricanalysis (TGA) was realized in an equipment Shimadzu DT-50 thermal analyzer while the X-ray photoelectron spectroscopy (XPS) measurements were carried out in a Kratos Axis Ultra Analyzer where all binding energies were referred to the C 1 s signal at 284.0 eV.

2.4 Batch adsorption test

To study the effect of several operational conditions on the DIF and IBF adsorption onto AC, batch adsorption tests were performed with 50 mL of deionized water (0.056 µS cm^{-1} Milli-Q) containing DIF or IBF at concentrations of 50 mg L^{-1} for 5 h and under constant agitation at 250 rpm. Initial pH of the solution was adjusted by using NaOH or HCl solutions (1 mol L^{-1}) until reach values of 3.0, 6.0, 9.0, and 12.0, at 25 ± 1 ºC and with an AC concentration of 1 g L^{-1}. The effect of the initial concentration of pollutants was carried out using values of 5, 15, 25, and 50 mg L^{-1} of either DIF or IBF with initial AC concentrations of 1 g L^{-1}, adjusting the initial pH according to the previous experiments. The effect of AC amount was evaluated by variating its concentration at 0.05, 0.25, 0.5, 0.75, and 1.0 g L^{-1}, adjusting the pH according to the previous experiments and keeping the temperature at 25 ± 1 ºC. The effect of temperature on pollutants adsorption was evaluated at 25, 35, 45, and 55 ± 1 ºC using the best conditions of pH, initial pollutant, and AC concentration. All the experiments were carried out in triplicate. The variation of IBF and DIF concentration in an aqueous solution was followed using the methodology reported by us employing a Perkin Elmer Lambda 35 UV–Vis spectrophotometer, USA [3]. The thermodynamic parameters for DIF and IBF adsorption on AC were evaluated using a range of adsorbate concentrations (i.e., from 5 mg L^{-1} to 100 mg L^{-1}) and different temperatures (i.e., 25 °C, 35 °C, 45 °C and 55 ± 1 °C) following Eqs. 1–3 where the thermodynamic equilibrium constant (K_C; dimensionless) was derived from the isotherm constant of Langmuir with linearized forms of Lineweaver–Burk [42, 43]. In order to evaluate the fitting of each isotherm model, the R-squared coefficient (R^2), nonlinear chi-square test (χ^2) and normalized standard deviation Δq (%) were calculated:

$$K_c = M_w * 55.5 * 1000 * K_L \quad (1)$$

$$\Delta G° = -RT \ln(K_c) \quad (2)$$

$$ln(K_c) = \frac{(T\Delta S° - \Delta H°)}{RT} \quad (3)$$

where the factor 55.5 is the number of moles of pure water per liter and term 55.5 × 1000 x K_L is dimensionless. ΔGº, ΔHº, ΔSº are the Gibbs free energy (kJ mol^{-1}), enthalpy (kJ mol^{-1}), and entropy (J mol^{-1} K^{-1}), respectively. The ideal gas constant (8.314 J mol-1 K^{-1}) and the absolute temperature (K) is R and T values, respectively. ΔSº and ΔHº were determinate from the intercept and the slope of the thermodynamic graph plot between ln (K_c) and 1/T.

2.5 Desorption and recycling experiments

The recycling of AC was assessed through the four adsorption–desorption cycles in controlled pH conditions, initial concentration of IBF or DIF, activated carbon dose, and temperature according to optimization batch experiment (agitation time of 1 h and magnetic agitation 250 rpm). After each adsorption cycle, 3 different solvents (acetonitrile, ethanol, and NaOH at concentrations of 5, 10, 15, 25, and 40% v.%) were used to achieve the pollutants desorption. Desorption experiments were carried out by washing the AC three times followed by rinsing with deionized water and drying at 80 ºC for 24 h.

2.6 Optimal adsorption conditions of DIF and IBF onto activated carbon in natural groundwater samples

Natural groundwater samples were obtained from a well located in a peri-urban community near to the city of La Plata (Argentina). The physicochemical features of natural groundwater are summarized in Table 1. Optimization of adsorption processes was studied by using a response surface methodology (RSM) of type central composite experimental design (CCD) – 2^3 in 3 blocks with triplicates generating seventeen experimental runs for each pollutant. The CCD was performed employing Statgraphics Centurion XVI software (version 16.1.03) as shown in Table 2 where amounts of AC (0.3 – 1 g L^{-1}), initial pH values (4 – 10), and initial concentration of IB or DI (6.5 – 25 mg L^{-1}) were chosen as experimental factors and evaluated at contact times of 90 min. The optimal conditions were employed to carry out the recycling adsorption experiments. Finally, the effect of ions such as nitrate (at concentrations ranging from 10 to 40 mg L^{-1}), bicarbonate (at concentrations ranging from 300 to 600 mg L^{-1}) and sulfates (at concentrations ranging

Table 1 Physicochemical characterization of natural groundwater samples

Parameters	Results	Units
Alkalinity	409.2	mg L^{-1} $CaCO_3$
Arsenic	0.04	mg L^{-1}
Electric conductivity	961	µS cm^{-1}
pH	8.0	
Calcium	7.90	mg L^{-1}
Total hardness	37.4	mg L^{-1} $CaCO_3$
Fluoride	1.03	mg L^{-1}
Total phosphorus	0.11	mg L^{-1}
Nitrate	17.69	mg NO_3^- L^{-1}
Nitrite	< 0.030	mg NO_2^- L^{-1}
Sulfate	4.73	mg L^{-1}

Table 2 Experimental design of central composite design (CCD) 2^3 in 3 blocks for the optimal adsorption of ibuprofen and diclofenac under natural groundwater

Factors		**Levels**				
		Axial point (-α)	Low (-)	Central point (0)	High (+)	Axial point (+α)
×*1*: amount of AC (g L^{-1})		0.064	0.3	0.65	1	1.23
×*2*: pH		1.98	4	7	10	12
×*3*: initial concentration of DIF/IBF (mg L^{-1})		0.271	6.5	15.75	25	31.22
Run	×*1*	×*2*	×*3*	**Response variables**		**Units**
1	+	-	+			
2	-	-	-			
3	+	+	-			
4	-	+	+	$R_{(DIF / IBF)}$		%
5	0	0	0			
6	+	+	+			
7	-	-	+			
8	-	+	-			
9	+	-	-			
10	0	0	0			
11	+α	0	0			
12	-α	0	0			
13	0	+α	0			
14	0	0	0			
15	0	0	-α			
16	0	-α	0			
17	0	0	+α			

from 4 to 10 mg L^{-1}) which are often present in natural groundwater samples, on the DIF and IBF adsorption was studied in deionized water.

3 Results and discussion

3.1 Characterization of activated carbon from raw seed shell

Physicochemical characterization of synthesized AC was performed by SEM–EDS, TGA/DTG, FT-IR, Raman-FT, and XPS (Fig. 1). SEM micrographs (Fig. 1a) revealed well-defined porous and channel structures while EDS measurements showed the elemental composition of the activated carbon surface detecting the presence of C, O, Si, and P. On the other hand, the FT-IR spectrum (Fig. 1b) exhibited bands at 1185 cm^{-1} probably assigned to the stretching of P = O bond in a phosphate ester or HO-P = O bond due to the formation of phosphate and pyrophosphates coming from the activating agent [3, 50]. Additionally, bands at 468 cm^{-1} are probably associated with symmetric stretching of PO_4^{3-} and C = O groups [17]. The presence of several signals corresponding to carbonaceous species was also observed. For instance, bands in the region between 3000–2850 and 3500–3200 cm^{-1} could be assigned to the C-H stretching of alkanes and O–H of alcohols/phenols, respectively. Those bands at 1600 cm^{-1} could be associated with the stretching vibration of aromatic groups (C = O, C = C) [3, 12, 13, 21]. This inclusion of oxygenated groups (O–H, C = O, and phosphorus-containing) on the surface of the activated carbon has been linked to possible adsorption sites of DIF and IBF, i.e., the O–H groups can function as H-bonders, and the O atoms of the organic contaminants act as promoters, which facilitates adsorbent-drug interaction through H-bonding. [31, 47]. Deconvoluted XPS spectrum of P2p (Fig. 1c) revealed two peaks at BE of 134.2 ± 0.3 eV and 133.4 ± 0.3 eV assigned to the presence of functional groups C-O-P (such as $(CO)_3$-PO, $(CO)_2$-PO(OH) and (CO)—$PO(OH)_2$) and C-$PO(OH)_2$ or C_2-PO(OH) groups, respectively [40, 48]. The C1s spectrum (Fig. 1d) of this material exhibited peaks related to O-C = O, C = O, C-O–O, and π-π* shake-up of carbonaceous species [3]. The C = O, π-π*, and P = O groups can be associated as common π-π and n-π (donor–acceptor) active interaction sites that can interact with the drugs [31]. Similarly, the presence of aromatic groups -CO = , -P = O, C = C (electron-rich) and carboxyl groups (COO-) (as confirmed by FTIR and XPS). These functionalities can act as π and n electron donor sites to form π-π interactions between these π electron donor sites and the pollutants, which act

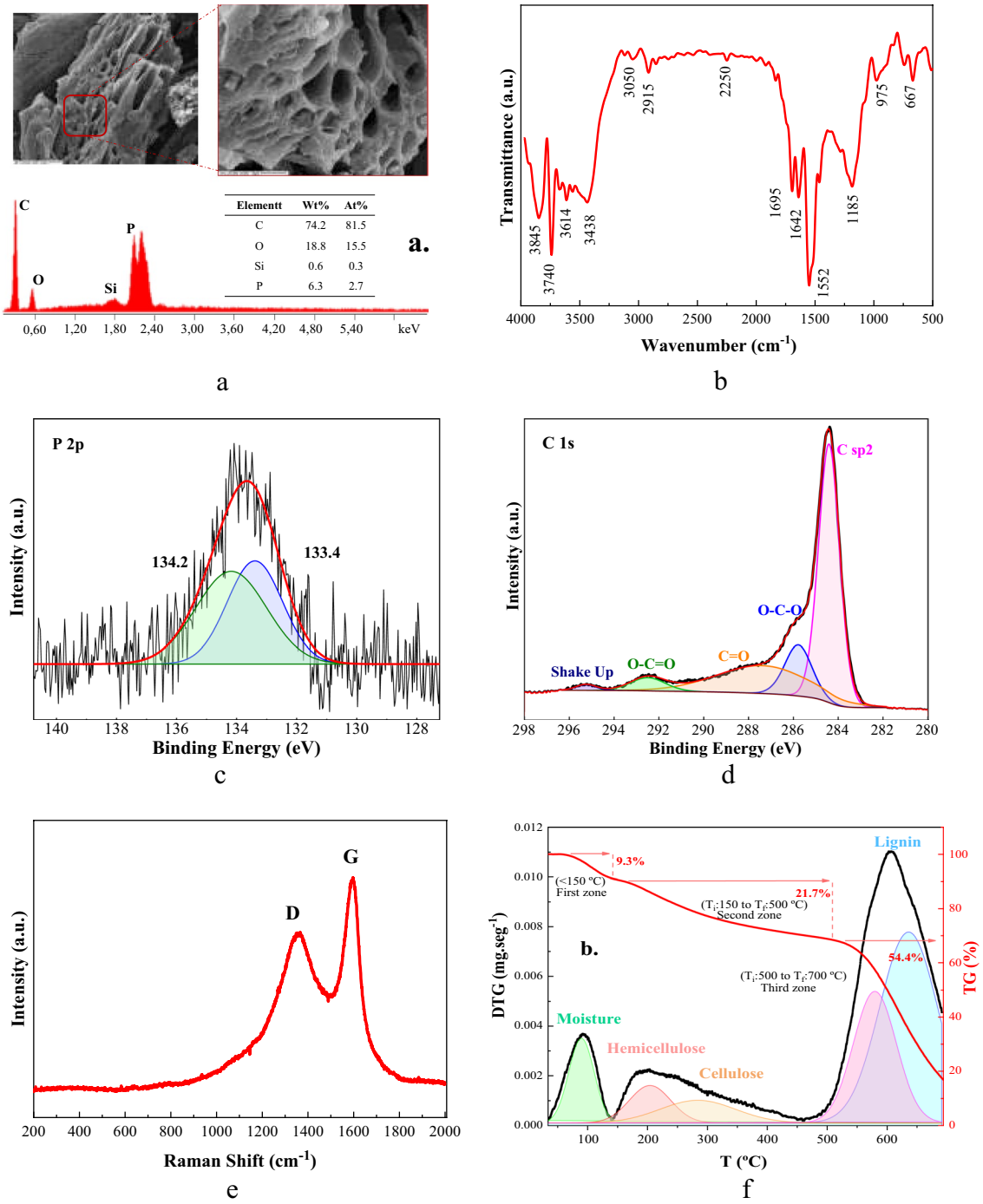

Fig. 1 Multi-technique characterization of activated carbon from SSS, **a**) scanning electron microscopy with energy dispersive X-ray spectroscopy—SEM/EDX, **b**) Fourier transform infrared spectroscopy—FTIR, **c**) X-ray photoelectron spectroscopy—XPS spectrum P 2p, **d**) spectrum XPS C 1 s, **e**) Raman-FT spectrum, and **f**) differential thermal analysis—DTG and thermogravimetric analysis—TG

as π electron acceptors (benzene ring) at adsorbate–adsorbate interface [14]. The Raman spectrum (Fig. 1e) shows the characteristic peaks at approximately 1360 and 1600 cm^{-1} associated with the D and G bands characteristic of disordered structural vibrations and vibration in sp2 graphitized carbon [49]. In addition, the ID/IG intensity ratio of 0.76 indicates a partially graphitized activated carbon surface, which would indicate possible sites conformed by aromatic structures available for π-π interactions [47].

The XPS and FT-IR characterization would confirm that AC exhibits surfaces highly functionalized with the presence of functional groups attributed to quinones, phenols,

aromatic compounds, and graphitic species coming from the partial degradation of lignin [3]. This could be confirmed for the thermogravimetric analysis (TGA) and its derivative thermogravimetry (DTG) curves for the SSS pre-treated with H_3PO_4 (Fig. 1f). These figures exhibited three thermal decomposition zones, which may be associated with the removal of moisture (< 150 °C); thermal hemicellulose and cellulose degradation between (150 to 500 °C), and lignin thermal decomposition (from 500 to 700 °C). At the carbonization temperature where the AC was synthesized (544 °C), TGA analysis revealed that lignin (W_{loss} of 4.4%) could be partially degraded in this material.

Textural characterization realized by N_2 adsorption–desorption isotherms revealed that AC shows a specific surface area of 1531 $m^2\ g^{-1}$, a pore volume of 0.98 $cm^3\ g^{-1}$, and a pore size of 5.5 nm. In our previous study [3], AC shown a type IV isotherm and H3 hysteresis, suggesting a mesoporous structure. This highly porous, phosphorus-modified structure promotes the arrangement of more active sites (P and O) on the surface of the AC. We found by titration with n-butylamine the presence of strong acid sites (E_i = 458 mV see the acid site classification in [3], and through Z-potential measurements, a point of zero charge (ZPC) value of 4.2. These results also indicated acid functionality at the surface of AC.

3.2 Adsorption experiments and the effect of parameters such as initial pH, temperature, initial concentration of pollutant, and AC dose

To study the adsorbent capacity of synthesized activated carbon, several parameters affecting the DIF and IBF adsorption, such as the initial pH of the solution, initial concentration of pollutants, AC dose, and temperature, were evaluated (Fig. 2).

Figure 2(a and b) shows the change in the normalized concentration (C/C_0) of DIF and IBF at pH in the range 3.0 -12.0 for an C_0 = 50 mg L^{-1} for both pollutants and a solution temperature of 25 ± 2 °C. Removal efficiencies at pH 3.0, 6.0, 9.0, and 12.0 was of 0.86, 0.7, 0.48, and 0.25% for DIF and 0.98, 0.7, 0.53, and 0.26% for IBF, respectively. It was also found that the removal efficiency of both molecules strongly decreased with pH increasing. The physicochemical properties of both pharmaceuticals (diclofenac (S_w = 2.37 mg L^{-1}; $LogK_{ow}$ = 4.51 and pK_a = 4.15) and ibuprofen (S_w = 21 mg L^{-1}; $LogK_{ow}$ = 3.79 and pK_a = 4.91)) suggest that at pH values of 6.0, 9.0, and 12.0, the prevalence of the anionic or deprotonated species (DIF^- and IBF^-) (pH > pKa) and negatively charged AC surfaces (PZC 4.2) would promote repulsive electrostatic interactions [22, 30] negatively affecting the adsorption of both pollutants. Furthermore, at acidic pH values (3.0), other interactions between contaminants and carbon surface such as π-π and hydrophobic interactions could be promoted. The above mentioned was also observed by Bhadra et al., where the diclofenac adsorption on commercial activated carbon was evaluated at low pH values. Authors suggested that under these experimental conditions, the surface of AC is protonated or positively charged while DIF molecule is also protonated (pH < pK_a) [7]. Since both IBF and DIF molecules possess carbon oxygenated functional groups hydrogen bonding as could be a possible mechanism explaining its adsorption on AC [7] (Scheme 1).

The influence of DIF and IBF concentration (5–50 mg L^{-1}) on the pollutants adsorption at pH 3.0 and 25 ± 2 °C was presented in Fig. 2(c and d). The removal curves dropped sharply in the initial stage (about 30 min), indicating that AC offers readily accessible sites for the substrate adsorption. It was also found that at low initial concentrations (5 mg L^{-1}), the time required for the complete adsorption of both pollutants was the lowest (60 min). The effect of the adsorbent dose on DIF and IBF removal was also evaluated at pH 3.0, pollutants initial concentration of 5.0 mg L^{-1}, and 25 ± 2 °C. Results revealed that by lowering the AC concentration, the pollutants adsorption strongly drops (Fig. 2e and f). However, in spite that AC concentrations of 1.0 g L^{-1} showed high effectiveness in the removal of both molecules, it was found that 0.5 g L^{-1} was the optimal AC dose considering 60 min of contact time and adsorption capacity of 9.35 mg g^{-1} (Q_{DI}) and 9.50 mg g^{-1} (Q_{IB}) as shown in the Figure S1(a and b). The adsorption rate does not show significant differences when the maximum amount of adsorbent was used (1.0 g L^{-1}), however, the amount of adsorbed pollutant per unit mass increased. The effect of temperature on the adsorption of DIF and IBF is shown in Fig. 2g and h. Results indicated that raising the temperature to 45 and 55 °C decreased the AC adsorption efficiency of both pollutants. This decrease could be related to the breakdown of weak adsorption interactions (Van der Waals forces and hydrogen bonding) due to the rising of the temperature [29]. Maximum adsorption efficiency was obtained at 35 ºC to DIF and IBF since probably, at this temperature there would be low aggregation and high diffusion of pharmaceutical compounds [1].

The adsorption isotherms obtained at 25 °C, 35 °C, 45 °C and 55 °C under the optimal adsorbent dose of 0.5 g L^{-1}, initial pH 3.0 during 24 h of continuous stirring were fitted to Langmuir and Freundlich isotherm model (Fig. 3). The Langmuir model presented the best statistical data fit. This was proven with the high R^2, and low Δq (%) and χ^2 values (Table 3 and S1) with a maximum adsorption capacity of 79.4 mg g^{-1}, 90.9 mg g^{-1}, 54 mg g^{-1}, 42.9 mg g^{-1} and 60.9 mg g^{-1}, 76.9 mg g^{-1}, 54.9 mg g^{-1}, 46.1 mg g^{-1}, for DIF and IBF respectively. The maximum adsorption capacities decreased by increasing the temperature.

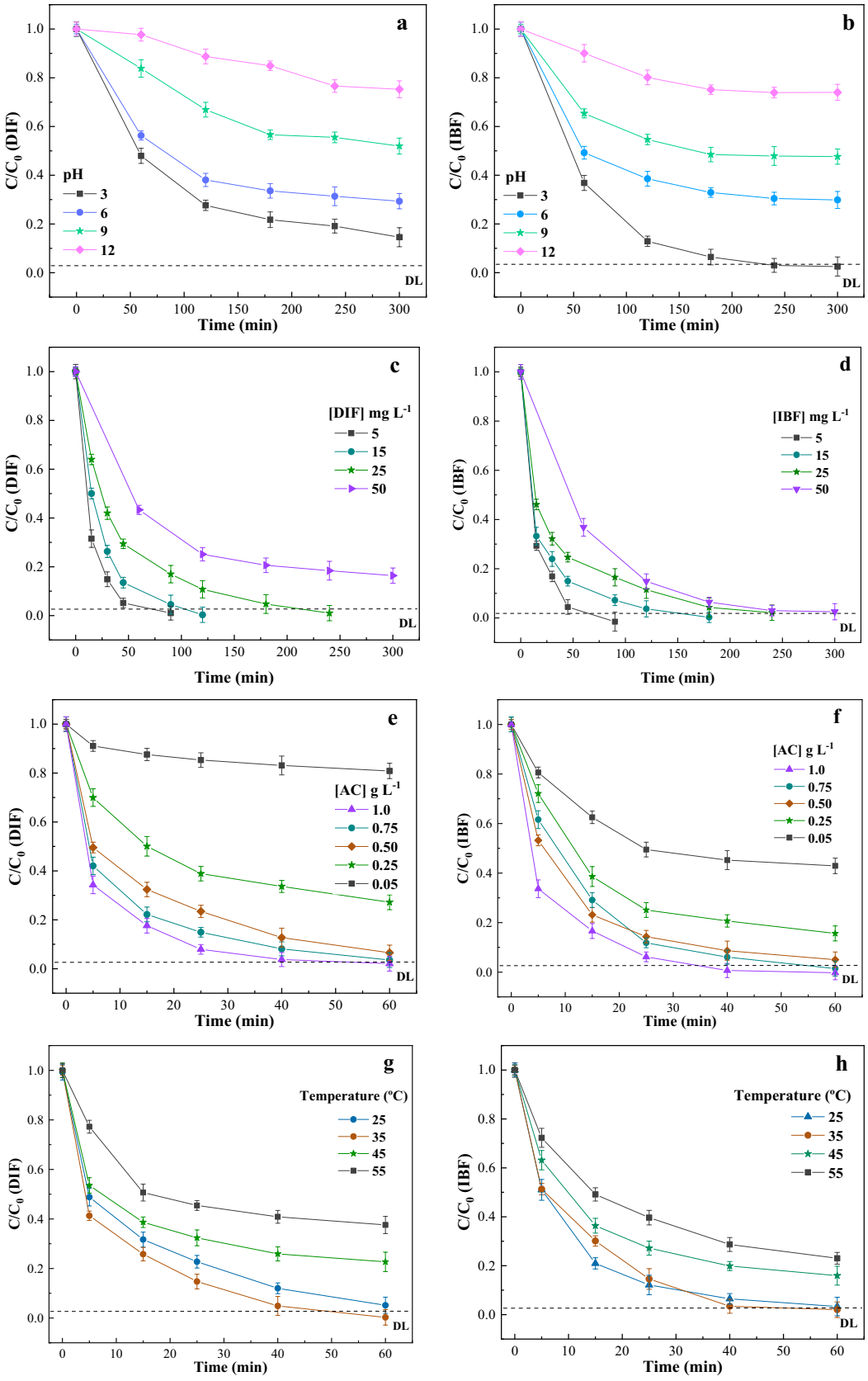
a
C/C0 (DIF)
Time (min)
pH
3
6
9
12
DL
b
C/C0 (IBF)
Time (min)
pH
3
6
9
12
DL
c
C/C0 (DIF)
Time (min)
[DIF] mg L-1
5
15
25
50
DL
d
C/C0 (IBF)
Time (min)
[IBF] mg L-1
5
15
25
50
DL
e
C/C0 (DIF)
Time (min)
[AC] g L-1
1.0
0.75
0.50
0.25
0.05
DL
f
C/C0 (IBF)
Time (min)
[AC] g L-1
1.0
0.75
0.50
0.25
0.05
DL
g
C/C0 (DIF)
Time (min)
Temperature (°C)
25
35
45
55
DL
h
C/C0 (IBF)
Time (min)
Temperature (°C)
25
35
45
55
DL

◂**Fig. 2** Effect of operational condition on DIF and IBF adsorption (**a** and **b**) the effect of pH, (**c** and **d**) the effect of initial concentration, (**e** and **f**) the effect of the amount of AC, and (**g** and **h**) the effect of temperature to DIF and IBF, respectively. Experimental condition: deionized water (0.056 µS cm^{-1}), volume solution 50 mL, amount activated carbon of 1 g L^{-1}, and stirring at 250 rpm

The thermodynamic parameters were calculated from the experimental data (Table 4). The ΔG° values of DIF and IBF adsorption onto AC gradually decreased with the temperature rising. In addition, negative values of ΔG° imply that adsorption of both pollutants under optimized conditions proceeded spontaneously [29, 35]. As described above, temperature raising has an important effect on the adsorption capacity of both pharmaceuticals. The absorption capacity (Q_{eq}) decreased from 79.4 mg g^{-1} at 25 °C (298 K) to 42.9 mg g^{-1} at 55 °C (328 K) and from 60.9 mg g^{-1} at 25 °C (298 K) to 46.1 mg g^{-1} at 55 °C (328 K) under equilibrium conditions for DI and IB, respectively. Similar results were reported for the adsorption of diclofenac and other pharmaceutical compounds onto carbon [4, 19, 23]. In addition, the calculated ΔH° values less than 40 kJ mol^{-1} could indicate physisorption rather than chemisorption (physisorption: ΔH° values < 40 kJ mol^{-1} and chemisorption: ΔH° values ≥ 40 kJ mol^{-1}) whereas negative values indicate that the adsorption phenomenon was exothermic [29, 36]. These observations were already described in our previous study where different interactions between AC and pharmaceuticals (DIF and IBF) were discussed suggesting that physisorption interactions such as the formation of hydrogen bonds, π-π, and hydrophobic interactions may play the main role in the adsorption of both pollutants onto the AC [3]. Moreover, a positive value of ΔS° could suggest that the randomness at the solid–liquid interface increased during the adsorption process which is a consequence of the structural changes in the interface [15]. This could be associated with the redistribution of DIF and IBF molecules adsorbed on the surface of AC, and as a result, the system may gain entropy.

3.3 Desorption and recycling experiments

The recyclability of activated carbon is an essential parameter for evaluating the material as a potential commercial and sustainable adsorbent. DIF and IBF were initially desorbed using water solutions containing 5 to 40% (v/v) of ethanol, NaOH, or acetonitrile (ACN) and sequential washing steps under continuous stirring. The desorption of both pharmaceuticals by different solution is presented in Figures S2 and S3. Results showed that acetonitrile solutions at 25 and 40% (v/v) ensured the most efficient desorption of both pollutants with a recovery percentage of around 85.6 and 89.6% for DIF and IBF, respectively. In this manner, the adsorbent could be reused for the next cycle. Four recycling tests were performed for both pharmaceuticals as shown in Fig. 4(a and b) the washing was according to the optimized conditions obtained. Depending on the properties of the adsorbates, regeneration take plane through a chemical reaction or pH change in the medium containing the AC [33]. The removal of pollutants with NaOH solutions can produce soluble salts (i.e., DIF as in Eq. (4) and IBF as in Eq. (5)). Also, the adsorbates are removed when the surface of ACs are negatively charged due to the high pH of the medium, and the intensification of repulsive forces between the anionic molecules adsorbed and the carbon surface breaks the adsorbent-adsorbate bonds [33].

$$C_{14}H_{10}C_{12}NOOH + NaOH \rightarrow C_{14}H_{10}C_{12}NN_aO_2 + H_2O \quad (4)$$

$$C_{13}H_{17}O_2Na + NaOH \rightarrow C_{13}H_{17}O_2Na + H_2O \quad (5)$$

Although the greater percentage removal is developed at high concentration. These experiments set showed that a very high NaOH concentrations, the removal efficiency decrease whit increase the number of reuses due to OH^- groups could be strongly retained on the active sites and hinders the subsequent adsorption step [26].

The effect of organic solvent depends mainly on the values of polarity that enhance the dipole and hydrogen-bonding interactions with the molecule of DIF or IBF. Although, after four reuse adsorption test activated carbon still exhibited high DIF and IBF adsorption (91.5% and 82%, respectively), a slight drop in the removal efficiency was observed possibly due to blockage of adsorbent micro-pores that decreases available adsorption sites [38]. the specific surface area, as shown in Figure S4, where this item underwent a reduction from 1531 m^2 g^{-1} (pristine activated carbon) to 1335 m^2 g^{-1} after four reusing cycles. This shown a significant decrease in the activated carbon surface area producing a detrimental effect on its textural features.

3.4 Optimal adsorption condition on natural groundwater matrices

The performance of the activated carbon as adsorbent of DIF and IBF in real groundwater samples was evaluated. The experiments were carried out using a response surface (RMS) methodology of type central composite design (CCD) to determine the optimal conditions for DIF and IBF adsorption. Table 1 shows the physicochemical features of groundwater samples analyzed according to Standard Methods (APHA/AWWA/WEF 2012). The pH (8.0) of the groundwater sample indicates slightly alkaline values, while alkalinity of 409.2 mg L^{-1} $CaCO_3$ and electric conductivity around 961 µS cm^{-1} suggested an important presence of salts and ions (nitrate, calcium, sulfate, and carbonates among others).

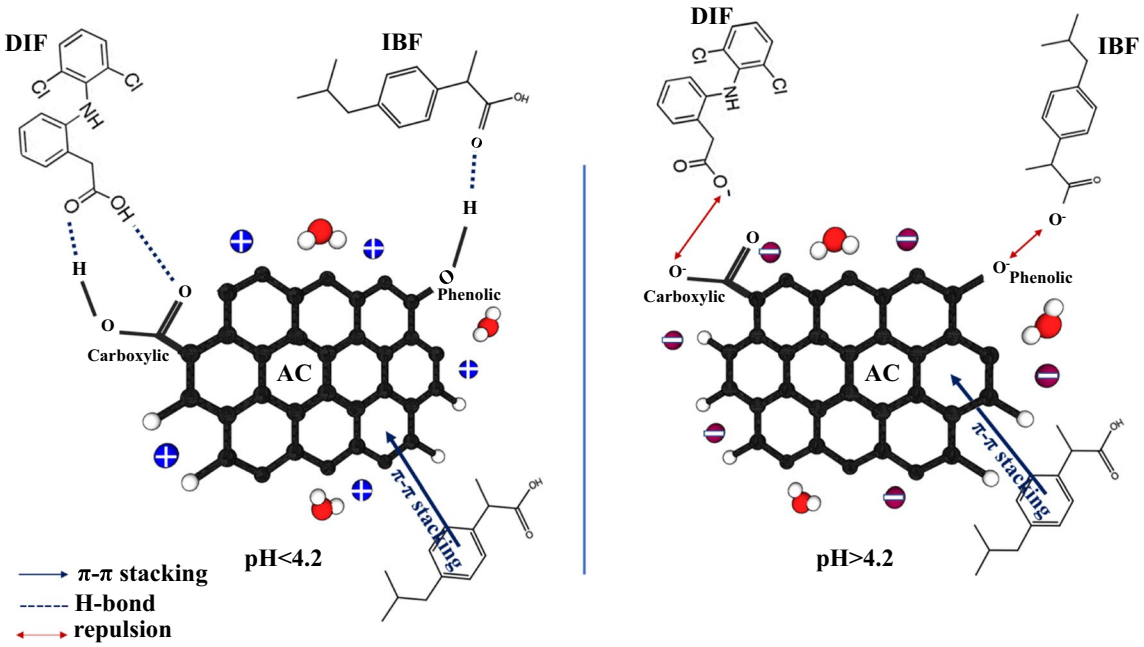

Scheme 1 Suggested IBF and DIF adsorption mechanisms on activated carbon

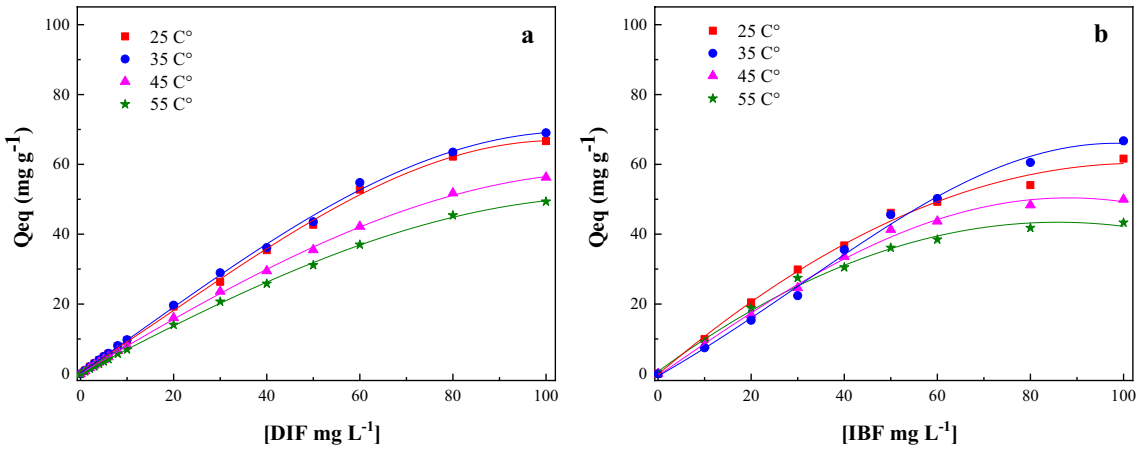

Fig. 3 Adsorption isotherms at different temperatures: (**a**) DIF and (**b**) IBF. (C_0 = 1 – 100 mg L^{-1}, AC dosage = 0.5 g $L.^{-1}$, equilibration time = 60 min)

According to the CCD matrix, experiments were carried out in triplicate presenting the experimental design and results in Tables S2 and S3. The analysis of variance ANOVA (Tables S4 and S5) showed that the R-squared (R^2) describing the correlation between experimental data and experimental factors (pH, AC dose, and [IBF] or [DIF]) were 0.94 and 0.97 for removal of DIF and IBF, respectively confirming that the model was statistically significant. Only 8% and 3% of the total variance is not explained by the 2^3 CCD model (after 45 min of contact time). Moreover, results indicated that the quadratic model exhibited a higher determination of coefficient (R^2). Figures 4 and 5 show the response surface plots at several initial concentrations of DIF and IBF.

The effect of initial solution pH and activated carbon dose on the adsorption of different initial concentrations of DIF was shown in Fig. 5(a–c). The optimal ranges of pH and AC dose were around 6.0–9.0 and 0.6–1.0 g L^{-1}, respectively to low and medium initial concentrations of pollutant (6.5 and 15.75 mg L^{-1}) obtaining removals close to 85 and 94%. On the other hand, it was observed that DIF removal increased with an AC dose in the range of 1.0 – 1.5 mg L^{-1} and an

Table 3 Thermodynamic parameters for adsorption of diclofenac (DIF) and ibuprofen (IBF) on AC. Experimental condition: deionized water (0.056 µS cm^{-1}), volume solution 50 mL, amount of activated carbon 0.5 g L^{-1}, contact time 24 h, initial concentration of DIF and IBF of 1 -100 mg L^{-1}, pH of 3.0, and stirring at 250 rpm

Isotherms Langmuir	Parameters	Temperature (°C)			
		25	35	45	55
DIF	Q_{eq} (mg g^{-1})	79.36	90.90	54.05	42.91
	K_b (L mg^{-1})	0.180	0.116	0.096	0.069
	R^2	0.99	0.98	0.98	0.97
	Δq(%)	2.04	1.74	2.81	3.04
	χ^2	0.089	0.12	0.87	0.34
IBF	Q_{eq} (mg g^{-1})	60.97	76.92	54.94	46.08
	K_b (L mg^{-1})	0.449	0.356	0.254	0.204
	R^2	0.98	0.99	0.97	0.99
	Δq(%)	1.1	2.7	1.8	2.8
	χ^2	0.097	0.105	0.52	1.2

initial pH solution ranging between 3.0 and 6.0 for values of DIF initial concentrations of 25 mg L^{-1}.

The significance of each experimental factor was assessed according to the *p*-value (where the *p*-value < 0.05 indicated that the model was significant). Pareto diagram (Fig. 6a) suggests that the factor C: [AC] at a high level, factor A: pH at a low level, the combined effect of factors AB, and the quadratic effect of pH (AA) had a significant impact on the removal of DIF. Figure 6b shows the main effects chart such as initial pH, initial DIF concentration, and AC dose on the pollutant removal in groundwater samples. This chart shows the negative effect of pH raising from 9.0 to 12.0. On the other hand, the DIF adsorption was negatively affected by the increase of initial pollutant concentration. As was described previously, it was observed that DIF adsorption was enhanced by increasing the AC dose. This highly probably could be due to the increasing of available sites on the activated carbon surface.

Regarding the IBF adsorption on AC in groundwater samples, the response surface (Fig. 7a-c) shows that the optimal pH range was around 6.0–9.0 for all the different initial concentrations of pollutant. Response surfaces at low and medium initial concentrations (6.5 and 15.75 mg L^{-1}) and activated carbon doses higher than 0.9 mg L^{-1} showed values of IBF removal between 90 and 80%, respectively. It was also observed that the removal of IBF strongly decreased at initial pollutant concentrations of 25 mg L^{-1}. The Pareto diagram

Table 4 Thermodynamic parameters for DIF and IBF

Pharmaceutical	Temperature (K)	ΔG° (kJ mol^{-1})	ΔH° (kJ mol^{-1})	ΔS° (J mol^{-1} K^{-1})	Van't Hoff equation
DIF	298	-36.93	-24.75	40.57	y = 2976.3x + 4.8793
	308	-37.04			R^2 = 0.98
	318	-37.76			
	328	-38.05			
IBF	298	-39.20	-22.02	57.70	y = 2648.6x + 6.9483
	308	-39.92			R^2 = 0.99
	318	-40.33			
	328	-40.99			

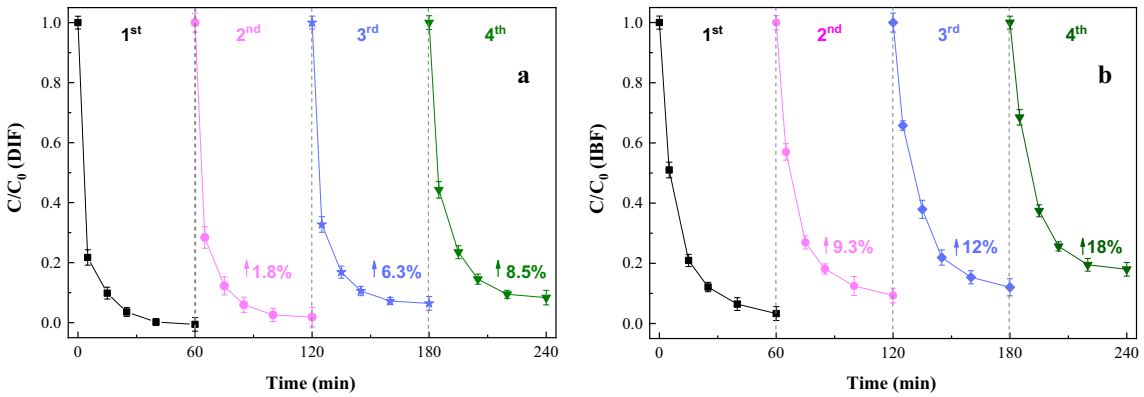

Fig. 4 The adsorption efficiency of pharmaceuticals during recycling experiments on AC, (**a**) DIF, and (**b**) IBF. Experimental condition: deionized water (0.056 µS cm^{-1}), pH of 3.0, temperature 25 ± 2 ºC, volume solution 50 mL, amount activated carbon of 0.5 g L^{-1}, and stirring at 250 rpm

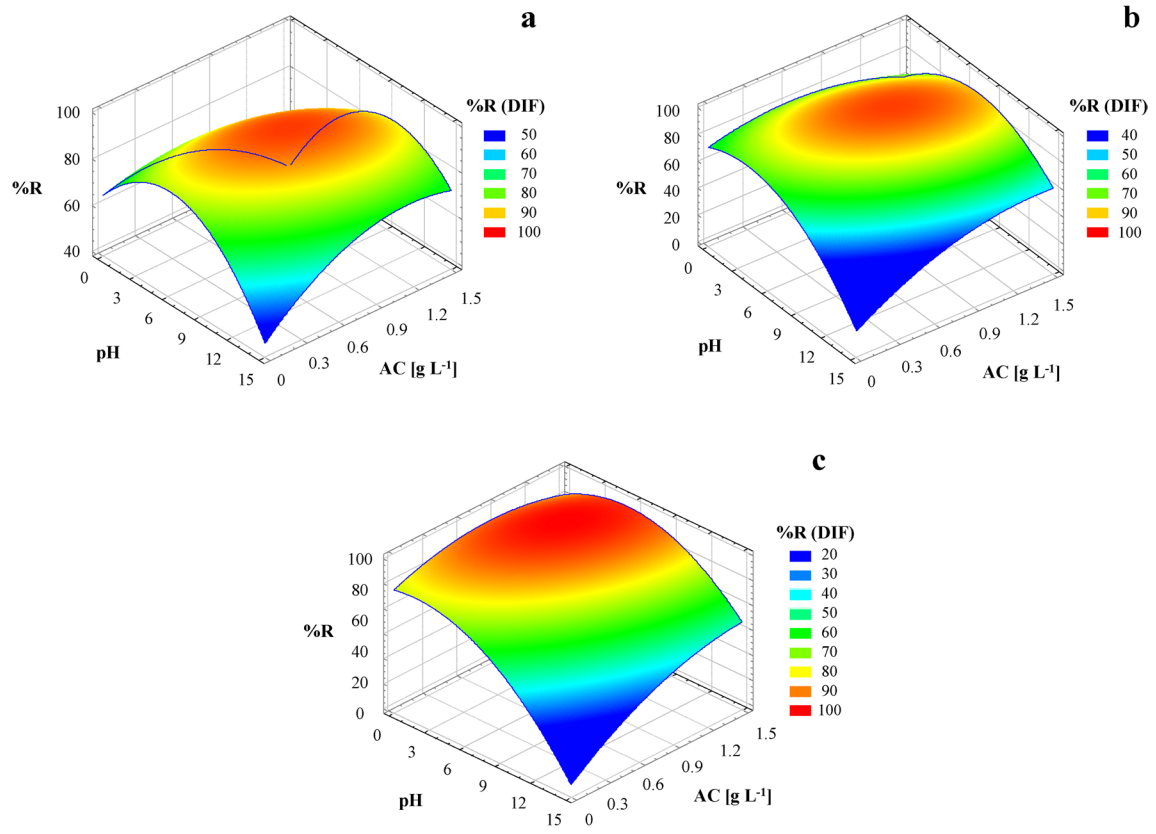

Fig. 5 Response surface plots of removal % of DIF by AC adsorption in natural groundwater ($R^2 = 0.94$), **a**.) 6.5 mg L^{-1}, **b**.) 15.75 mg L^{-1}, and **c**.) 25 mg L^{-1} of DIF initial concentrations. Experimental conditions: Temperature 25 ± 2 ºC, volume solution 50 mL, contact time of 45 min and stirring at 250 rpm

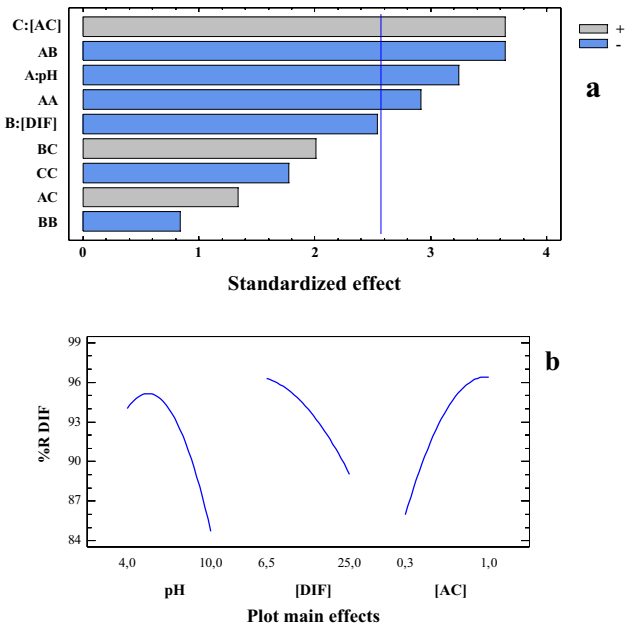

Fig. 6 **A**) Pareto and (**b**) main effects chart obtained from ANOVA analysis of DIF adsorption onto activated carbon in natural groundwater

(Fig. 8a) indicates that the factor C: [AC] at a high level positively affected IBF removal. The combined effect of factors B and C showed a significant result in the IBF adsorption when experimental values at low levels were used. Furthermore, the AA factor (quadratic effect of pH) presented the highest significant value at an experimental low level. The main effects chart (Fig. 8b) indicated the pH parameter (7.0) exhibited a positive impact on IBF removal at values near the central point of the experimental design. A slight negative effect was also observed on the IBF removal at high initial pollutant concentrations. Finally, AC dose showed a positive effect with increasing the activated carbon concentration.

The experimental data were fitted to a second-order response surface model [3]. The result exhibited the optimum condition for DIF and IBF adsorption in natural groundwater samples. Thus, the optimum condition for DIF adsorption would be the initial pH of 8.0, initial pollutant concentration of 6.5 mg L^{-1} and AC dose of around 0.79 g L^{-1}. On the other hand, IBF adsorption displayed optimal conditions at pH values of 7.0, AC dose of 1.0 g L^{-1}, and initial pollutant concentration of 6.5 mg L^{-1}. Reusing experiments were evaluated using these optimized experimental conditions.

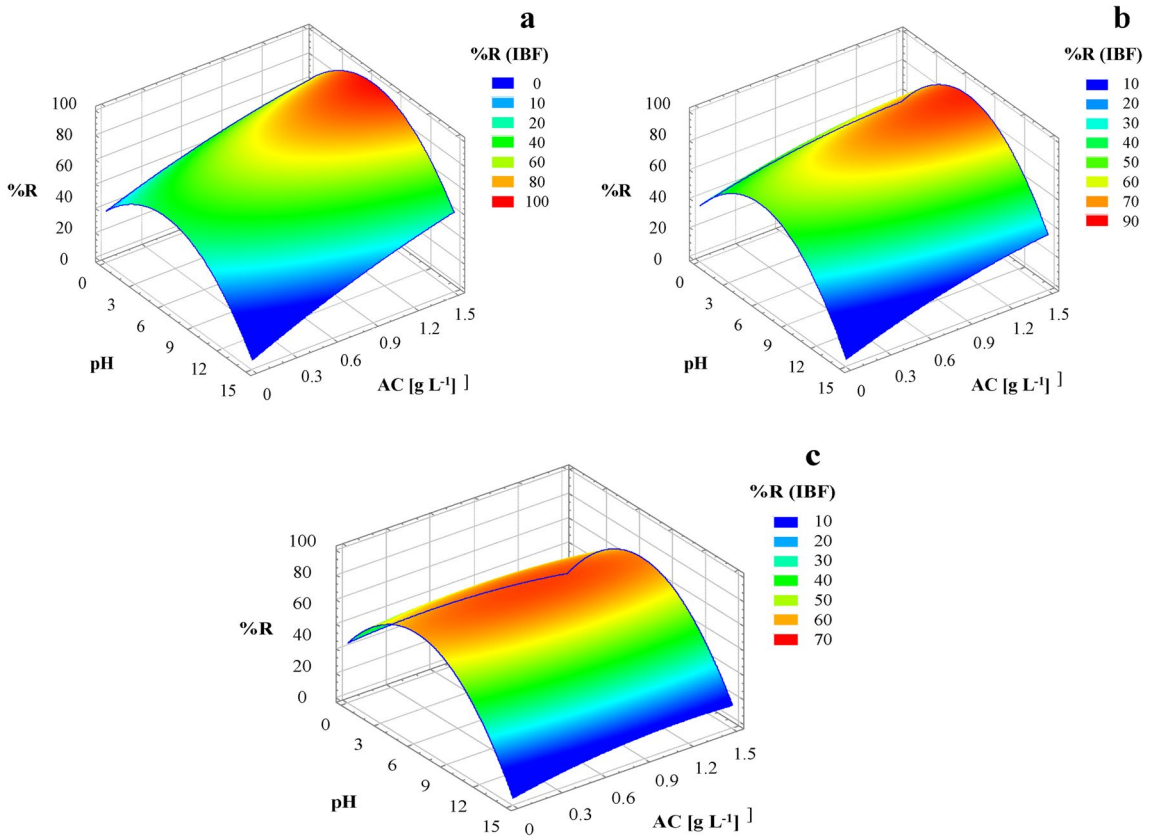

Fig. 7 Response surface plots of removal % of IBF by AC adsorption in natural groundwater ($R^2 = 0.96$), **a**.) 6.5 mg L^{-1}, **b**.) 15.75 mg L^{-1}, and **c**.) 25 mg L^{-1} of initial concentrations of DIF. Experimental conditions: Temperature 25 ± 2 ºC, volume solution 50 mL, contact time of 45 min, and stirring at 250 rpm

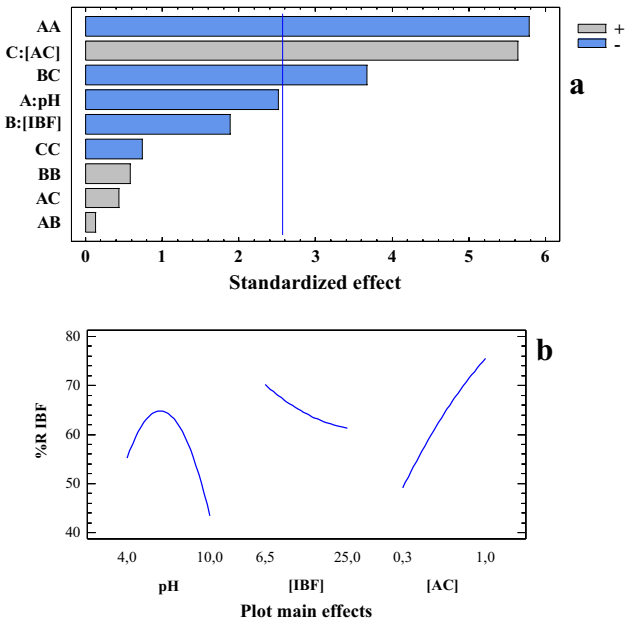

Fig. 8 Pareto and (**b**) main effects chart obtained from ANOVA analysis of IBF adsorption onto activated carbon in natural groundwater

The recyclability of activated carbon after desorption treatment in natural groundwater samples is shown in Fig. 9(a and b). Pollutants desorption was achieved using acetonitrile solutions at 25 and 40% (v/v), ensuring the most efficient pollutants desorption. Recycled AC showed a high adsorption capacity towards DIF and IBF even after four reuses, obtaining DIF and IBF removal values of 72% and 66%, respectively. However, after each adsorption–desorption cycle, the efficiency was reduced possibly due to the pore blockage effect of activated carbon [39]. Moreover, it was observed a higher reduction of adsorption capacity in natural groundwater samples compared with deionized water. This could be attributed to an adsorption competition between pollutants and ions in natural samples.

3.5 Study in deionized water of the effects of ions at concentrations typically found in natural waters on the adsorption of IBF and DIF onto activated carbon

Considering the chemistry of natural groundwater, the influence of some ubiquitous ions on DIF and IBF

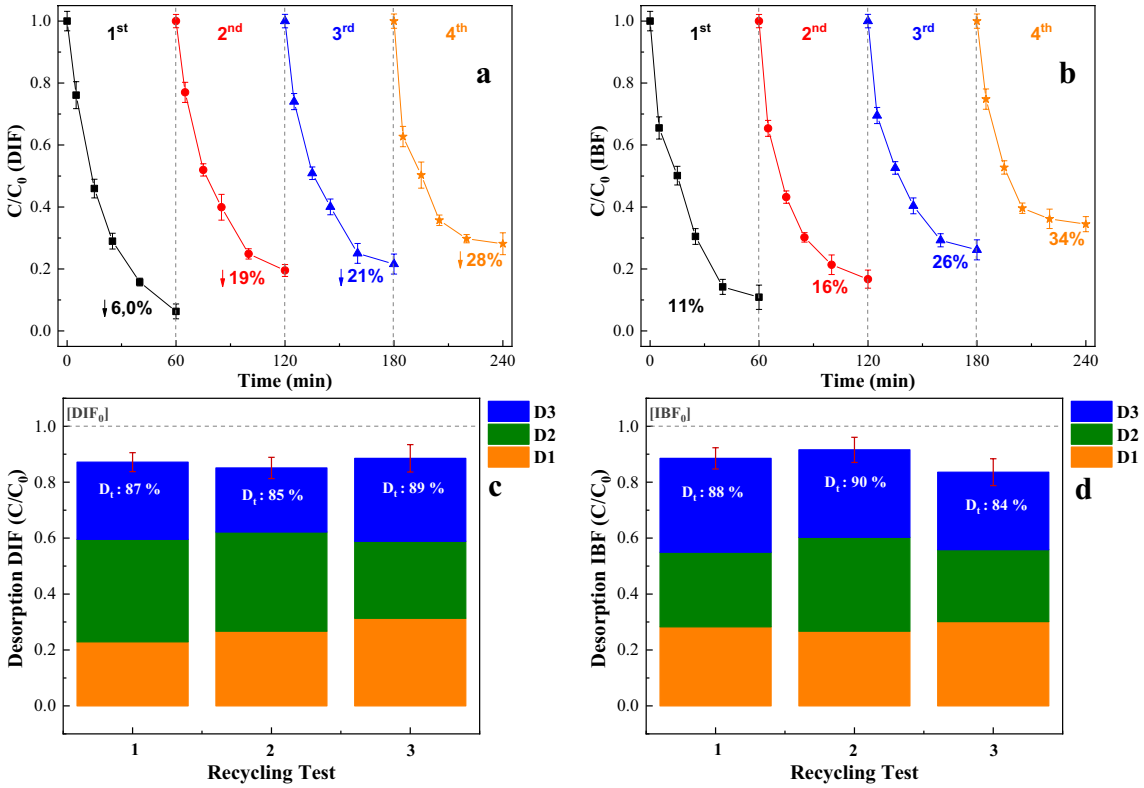

Fig. 9 The adsorption of pharmaceuticals onto activated carbon during recycling experiments in natural groundwater, (**a**) DIF and (**b**) IBF. Desorption procedure of DIF (**c**) and IBF (**d**) from activated carbon by using acetonitrile.water solutions (25% (v/v) for DIF and 40% (v/v) for IBF, respectively)

adsorption on AC was investigated in deionized water using anions at concentrations commonly found in natural waters. As shown in Fig. 10(a-f), IBF adsorption was strongly affected for the presence of anions (NO_3^-, SO_4^{2-}, HCO_3^-). On the other hand, DIF adsorption was only affected by the presence of the bicarbonate ions (HCO_3^-). The significant impact of these species on the adsorption of pharmaceutical compounds could be due to negatively charged layers formed by adsorbed anions that increase electrostatic repulsion between both DIF or IBF molecules and AC surface. Moreover, several authors have reported that bivalent anions such as SO_4^{2-} could reduce the solubility of DIF affecting its adsorption on activated carbons in deionized water [18, 39, 51] while hydrolysis of HCO_3^- anions would lead to a solution pH raising generating a detrimental effect on the pollutant adsorption as it was mentioned in Section 2.2.

4 Conclusions

Activated carbon synthesized from sunflower seed shells and activated with H_3PO_4 may provide future practical applications, exhibiting good textural properties (S_{BET}:1531 $m^2\ g^{-1}$) and chemical surface characteristics (O-C = O, C = O, C-O–O, C-O-P, and PO_4^{3-}) to be used as an adsorbent in the removal of diclofenac and ibuprofen from natural water samples. The desorption methodology (ACN:wáter solution of 25% and 40% for DIF and IBF) developed in this work allowed studying the regeneration of the adsorbent.

The results showed that non-ionized species of contaminants had the highest removal efficiencies of 86% and 98% (at pH 3) for solutions in deionized water. At these pH conditions, electrostatic interactions are unfavorable (AC maintained positively charged $pH < pH_{PZC}$). Thus, dispersive (π-π) interactions would explain the adsorption at this low pH. The Langmuir isotherm best described the adsorption equilibrium of each contaminant at all temperatures analyzed, while the thermodynamic analysis supported this suggestion since (ΔH°) values could indicate the participation of physisorption mechanisms (< 40 kJ/mol).

Experimental design methodology found the optimal experimental conditions such as activated carbon dose, initial concentration of DIF and IBF, and initial pH solution. Optimal values were 0.9 g L^{-1}, 6.5 mg L^{-1}, and 6.8, respectively, for DI adsorption, whereas IB adsorption

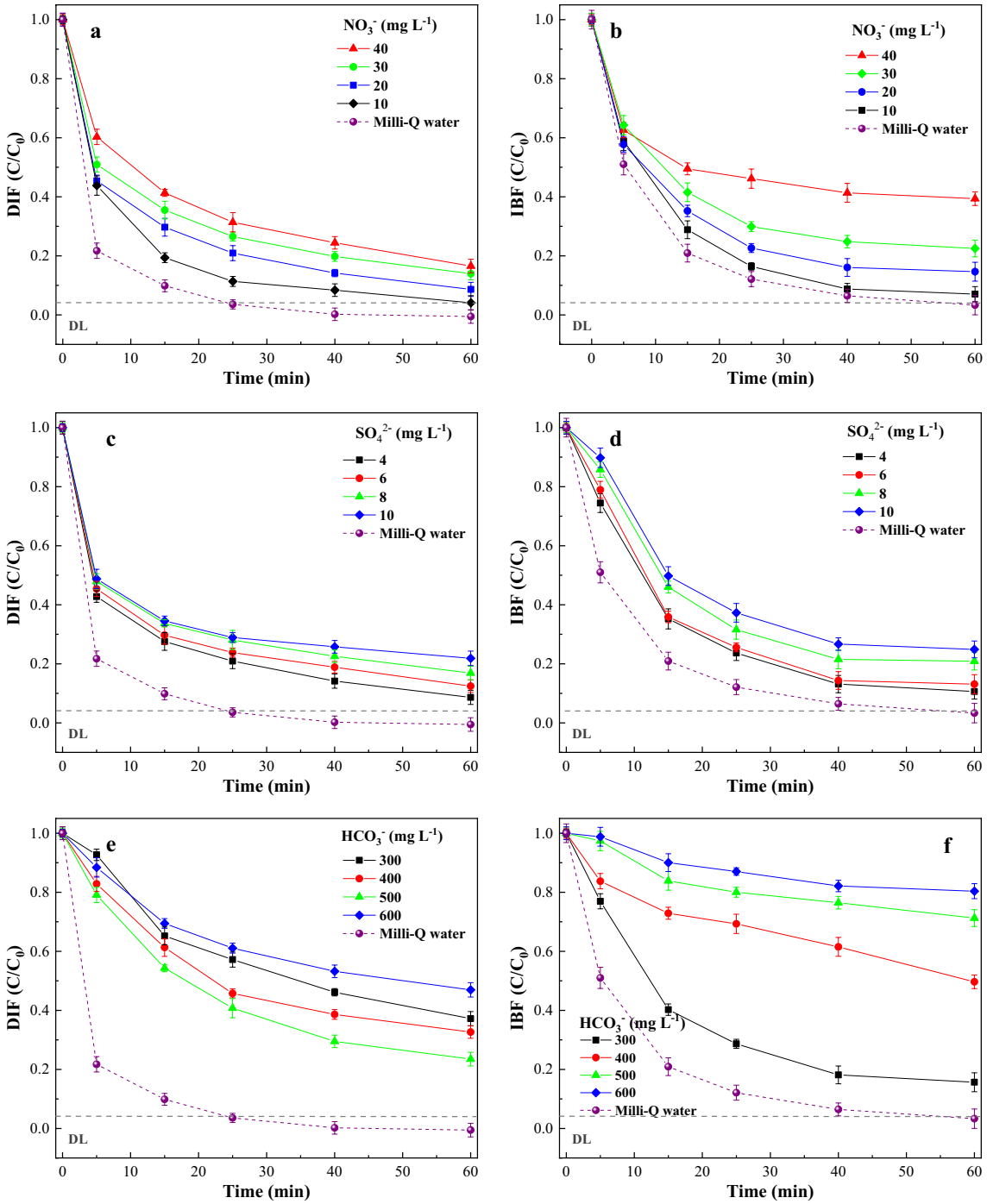

Fig. 10 Effect of nitrate ions (NO_3^-) on (**a**) DIF and (**b**) IBF adsorption. Effect of sulfate ions (SO4=) on (**c**) DIF and (**d**) IBF adsorption and effect of bicarbonate ions (HCO_3^-) on (**e**) DIF and (**f**) IBF adsorption. Experiments were performed in deionized water (0.056 μS cm^{-1}), pH 8.0 and AC concentration of 0.5 g L^{-1} at 25 °C

displayed optimal conditions at 7.5, 1.2 g L^{-1}, and 6.5 mg L^{-1}, respectively. On the other hand, AC shows an interesting potential for practical applications as an adsorbent in the treatment of waters polluted with DIF and IBF, exhibiting the capacity to be reused at least four times without significantly losing its adsorption capacity.

Supplementary Information The online version contains supplementary material available at https://doi.org/10.1007/s10450-024-00461-y.

Acknowledgements Authors thank to "Consejo Nacional de Investigaciones Científicas y Técnicas"-CONICET Argentina for the economic support (grant PIP 0449 and 1492) and National University of La Plata-UNLP and CONICET for the economic support (grant PIO 024).

Authors contributions JJAD: [Conceptualization, Methodology, Investigation, Formal Analysis, Visualization, Writing-original draft]. JARH: [Conceptualization, Methodology, writing review & editing, Supervision, Project Administration, and Funding Acquisition]. LRP: [Conceptualization, Methodology, writing review & editing, Supervision, Project Administration, and Funding Acquisition].

Funding "Consejo Nacional de Investigaciones Científicas y Técnicas"-CONICET Argentina for the economic support (grant PIP 1492). National University of La Plata-UNLP and CONICET for the economic support (grant PIO 024).

Data availability No datasets were generated or analysed during the current study.

Declarations

Ethical approval Not applicable.

Consent to participate and consent to publish All authors have read and approved the manuscript and they agree with the order of authors listed in the text.

Competing interests The authors declare no competing interests.

References

1. Ahmed, M.J.: Adsorption of non-steroidal anti-inflammatory drugs from aqueous solution using activated carbons: Review. J. Environ. Manage. **190,** 74–282 (2017). https://doi.org/10.1016/j.jenvman.2016.12.073
2. Álvarez-Torrellas, S., Rodríguez, A., Ovejero, G., García, J.: Comparative adsorption performance of ibuprofen and tetracycline from aqueous solution by carbonaceous materials. Chem. Eng. J. **283**, 936–947 (2016). https://doi.org/10.1016/j.cej.2015.08.023
3. Alvear-Daza, J.J., Cánneva, A., Donadelli, J.A., Manrique-Holguín, M., Rengifo-Herrera, J.A., Pizzio, L.R.: Removal of diclofenac and ibuprofen on mesoporous activated carbon from agro-industrial wastes prepared by optimized synthesis employing a central composite design. Biomass Convers. Biorefin. (2022). https://doi.org/10.1007/s13399-021-02227-w
4. Antunes, M., Esteves, V.I., Guégan, R., Crespo, J.S., Fernandes, A.N., Giovanela, M.: Removal of diclofenac sodium from aqueous solution by Isabel grape bagasse. Chem. Eng. J. **192**, 114–121 (2012). https://doi.org/10.1016/j.cej.2012.03.062
5. Baccar, R., Sarrà, M., Bouzid, J., Feki, M., Blánquez, P.: Removal of pharmaceutical compounds by activated carbon prepared from agricultural by-product. Chem. Eng. J. **211–212**, 310–317 (2012). https://doi.org/10.1016/j.cej.2012.09.099
6. Bhadra, B.N., Ahmed, I., Kim, S., Jhung, S.H.: Adsorptive removal of ibuprofen and diclofenac from water using metal-organic framework-derived porous carbon. Chem. Eng. J. **314**, 50–58 (2017). https://doi.org/10.1016/j.cej.2016.12.127
7. Bhadra, B.N., Seo, P.W., Jhung, S.H.: Adsorption of diclofenac sodium from water using oxidized activated carbon. Chem. Eng. J. **301**, 27–34 (2016). https://doi.org/10.1016/j.cej.2016.04.143
8. Bibi, M., Rashid, J., Malik, M., Iqbal, A., Xu, M.: Physico-chemical analysis and detection of exceptionally high diclofenac concentration in the pharmaceutical wastewaters collected from the production units of national industrial zone, Rawat, Pakistan. Appl. Water Sci. **13** (2023). https://doi.org/10.1007/s13201-023-01954-x
9. Bourassi, M., Kárászová, M., Pasichnyk, M., Zazpe, R., Hercik-ová, J., Fíla, V., Macak, J.M., Gaálová, J.: Removal of ibuprofen from water by different types membranes. Polymers (Basel). **13** (2021). https://doi.org/10.3390/polym13234082
10. Chang, C.F., Chen, T.Y., Chin, C.J.M., Kuo, Y.T.: Enhanced electrochemical degradation of ibuprofen in aqueous solution by PtRu alloy catalyst. Chemosphere **175**, 76–84 (2017). https://doi.org/10.1016/j.chemosphere.2017.02.021
11. Chen, H., Akhtar, L.: Chapter 3 - Fate and transport of pharmaceuticals and personal care products in soils and groundwater. In: Gao, B. (ed.) Emerging Contaminants in Soil and Groundwater Systems, pp. 49–82. Elsevier (2022). https://doi.org/10.1016/B978-0-12-824088-5.00004-5
12. Chen, M., He, F., Hu, D., Bao, C., Huang, Q.: Broadened operating pH range for adsorption/reduction of aqueous Cr(VI) using biochar from directly treated jute (Corchorus capsularis L.) fibers by H3PO4. Chem. Eng. J. **381**, 122739 (2020). https://doi.org/10.1016/j.cej.2019.122739
13. Chu, G., Zhao, J., Huang, Y., Zhou, D., Liu, Y., Wu, M., Peng, H., Zhao, Q., Pan, B., Steinberg, C.E.W.: Phosphoric acid pretreatment enhances the specific surface areas of biochars by generation of micropores. Environ. Pollut. **240**, 1–9 (2018). https://doi.org/10.1016/j.envpol.2018.04.003
14. Czech, B., Oleszczuk, P.: Sorption of diclofenac and naproxen onto MWCNT in model wastewater treated by H2O2 and/or UV. Chemosphere **149**, 272–278 (2016). https://doi.org/10.1016/j.chemosphere.2015.12.057
15. Díez, E., Gómez, J.M., Rodríguez, A., Bernabé, I., Sáez, P., Galán, J.: A new mesoporous activated carbon as potential adsorbent for effective indium removal from aqueous solutions. Microporous and Mesoporous Mater. **295** (2020). https://doi.org/10.1016/j.micromeso.2019.109984
16. di Lorenzo, T., Cifoni, M., Baratti, M., Pieraccini, G., di Marzio, W.D., Galassi, D.M.P.: Four scenarios of environmental risk of diclofenac in European groundwater ecosystems. Environ. Pollut. **287**, (2021). https://doi.org/10.1016/j.envpol.2021.117315
17. Iqbal, J., Mohamed Al Hajeri, B., Shah, N.S., Wilson, K., Xavier, C., Shaalan, J., Al-Taani, A.A., Howari, F., Nazzal, Y.: Preparation of H3PO4 modified Sidr biochar for the enhanced removal of ciprofloxacin from water. Int. J. Phytoremediation. **24**, 1231–1242 (2022). https://doi.org/10.1080/15226514.2021.2025038
18. Jiang, M., Yang, W., Zhang, Z., Yang, Z., Wang, Y.: Adsorption of three pharmaceuticals on two magnetic ion-exchange resins. J. Environ. Sci. (China) **31**, 226–234 (2015). https://doi.org/10.1016/j.jes.2014.09.035
19. Jodeh, S., Abdelwahab, F., Jaradat, N., Warad, I., Jodeh, W.: Adsorption of diclofenac from aqueous solution using Cyclamen persicum tubers based activated carbon (CTAC). J. Assoc. Arab Univ. Basic Appl. Sci. **20**, 32–38 (2016). https://doi.org/10.1016/j.jaubas.2014.11.002
20. Kumar, M., Jaiswal, S., Sodhi, K.K., Shree, P., Singh, D.K., Agrawal, P.K., Shukla, P.: Antibiotics bioremediation: Perspectives on its ecotoxicity and resistance, (2019)
21. Kundu, A., sen Gupta, B., Hashim, M.A., Redzwan, G.: Taguchi optimization approach for production of activated carbon from phosphoric acid impregnated palm kernel shell by microwave

heating. J. Clean. Prod. **105**, 420–427 (2015). https://doi.org/10.1016/j.jclepro.2014.06.093
22. Larous, S., Meniai, A.H.: Adsorption of Diclofenac from aqueous solution using activated carbon prepared from olive stones. Int. J. Hydrogen Energy **41**, 10380–10390 (2016). https://doi.org/10.1016/j.ijhydene.2016.01.096
23. Lonappan, L., Rouissi, T., Kaur Brar, S., Verma, M., Surampalli, R.Y.: An insight into the adsorption of diclofenac on different biochars: Mechanisms, surface chemistry, and thermodynamics. Bioresour. Technol. **249**, 386–394 (2018). https://doi.org/10.1016/j.biortech.2017.10.039
24. Ma, L., Liu, Y., Yang, Q., Jiang, L., Li, G.: Occurrence and distribution of Pharmaceuticals and Personal Care Products (PPCPs) in wastewater related riverbank groundwater. Sci. Total Environ. **821**, (2022). https://doi.org/10.1016/j.scitotenv.2022.153372
25. Malhotra, M., Suresh, S., Garg, A.: Tea waste derived activated carbon for the adsorption of sodium diclofenac from wastewater: adsorbent characteristics, adsorption isotherms, kinetics, and thermodynamics. Environ. Sci. Pollut. Res. **25**, 32210–32220 (2018). https://doi.org/10.1007/s11356-018-3148-y
26. Martin, R.J., Ng, W.J.: Chemical regeneration of exhausted activated carbon-I. Water Res. **18**, 59–73 (1984)
27. Mestre, A.S., Hesse, F., Freire, C., Ania, C.O., Carvalho, A.P.: Chemically activated high grade nanoporous carbons from low density renewable biomass (Agave sisalana) for the removal of pharmaceuticals. J. Colloid Interface Sci. **536**, 681–693 (2019). https://doi.org/10.1016/j.jcis.2018.10.081
28. Mestre, A.S., Pires, J., Nogueira, J.M.F., Parra, J.B., Carvalho, A.P., Ania, C.O.: Waste-derived activated carbons for removal of ibuprofen from solution: Role of surface chemistry and pore structure. Bioresour. Technol. **100**, 1720–1726 (2009). https://doi.org/10.1016/j.biortech.2008.09.039
29. Mondal, S., Aikat, K., Halder, G.: Biosorptive uptake of ibuprofen by chemically modified Parthenium hysterophorus derived biochar: Equilibrium, kinetics, thermodynamics and modeling. Ecol. Eng. **92**, 158–172 (2016a). https://doi.org/10.1016/j.ecoleng.2016.03.022
30. Mondal, S., Bobde, K., Aikat, K., Halder, G.: Biosorptive uptake of ibuprofen by steam activated biochar derived from mung bean husk: Equilibrium, kinetics, thermodynamics, modeling and ecotoxicological studies. J. Environ. Manage. **182**, 581–594 (2016b). https://doi.org/10.1016/j.jenvman.2016.08.018
31. Pap, S., Taggart, M.A., Shearer, L., Li, Y., Radovic, S., Turk Sekulic, M.: Removal behaviour of NSAIDs from wastewater using a P-functionalised microporous carbon. Chemosphere. **264**, (2021). https://doi.org/10.1016/j.chemosphere.2020.128439
32. Patel, M., Kumar, R., Kishor, K., Mlsna, T., Pittman, C.U. Jr., Mohan, D.: Pharmaceuticals of emerging concern in aquatic systems: chemistry, occurrence, effects, and removal methods. Chem. Rev. **119**, 3510–3673 (2019). https://doi.org/10.1021/acs.chemrev.8b00299
33. Salvador, F., Martin-Sanchez, N., Sanchez-Hernandez, R., Sanchez-Montero, M.J., Izquierdo, C.: Regeneration of carbonaceous adsorbents. Part II: Chemical, microbiological and vacuum regeneration. Micropor. Mesopor. Mat. **202,** 277–296 (2015). https://doi.org/10.1016/j.micromeso.2014.08.019
34. Saucier, C., Adebayo, M.A., Lima, E.C., Cataluña, R., Thue, P.S., Prola, L.D.T., Puchana-Rosero, M.J., Machado, F.M., Pavan, F.A., Dotto, G.L.: Microwave-assisted activated carbon from cocoa shell as adsorbent for removal of sodium diclofenac and nimesulide from aqueous effluents. J. Hazard. Mater. **289**, 18–27 (2015). https://doi.org/10.1016/j.jhazmat.2015.02.026
35. Shin, J., Kwak, J., Kim, S., Son, C., Lee, Y.G., Baek, S., Park, Y., Chae, K.J., Yang, E., Chon, K.: Facilitated physisorption of ibuprofen on waste coffee residue biochars through simultaneous magnetization and activation in groundwater and lake water: Adsorption mechanisms and reusability. J. Environ. Chem. Eng. **10**, (2022). https://doi.org/10.1016/j.jece.2022.107914
36. Shin, J., Kwak, J., Lee, Y.G., Kim, S., Son, C., Cho, K.H., Lee, S.H., Park, Y., Ren, X., Chon, K.: Changes in adsorption mechanisms of radioactive barium, cobalt, and strontium ions using spent coffee waste biochars via alkaline chemical activation: Enrichment effects of O-containing functional groups. Environ. Res. **199**, (2021). https://doi.org/10.1016/j.envres.2021.111346
37. Shirani, Z., Song, H., Bhatnagar, A.: Efficient removal of diclofenac and cephalexin from aqueous solution using Anthriscus sylvestris-derived activated biochar. Sci. Total Environ. **745**, (2020). https://doi.org/10.1016/j.scitotenv.2020.140789
38. Show, S., Karmakar, B., Halder, G.: Sorptive uptake of anti-inflammatory drug ibuprofen by waste biomass–derived biochar: experimental and statistical analysis. Biomass Convers. Biorefin. **12**, 3955–3973 (2022a). https://doi.org/10.1007/s13399-020-00922-8
39. Show, S., Karmakar, B., Halder, G.: Sorptive uptake of anti-inflammatory drug ibuprofen by waste biomass–derived biochar: experimental and statistical analysis. Biomass Convers. Biorefin. **12**, 3955–3973 (2022b). https://doi.org/10.1007/s13399-020-00922-8
40. Song, C., Chen, K., Chen, M., Jin, X., Liu, G., Du, X., Chen, D., Huang, Q.: Sequential combined adsorption and solid-phase photocatalysis to remove aqueous organic pollutants by H3PO4-modified TiO2 nanoparticles anchored on biochar. J Water Process Eng. **45**, 102467 (2022). https://doi.org/10.1016/j.jwpe.2021.102467
41. Torrellas, S.Á., GarcíaLovera, R., Escalona, N., Sepúlveda, C., Sotelo, J.L., García, J.: Chemical-activated carbons from peach stones for the adsorption of emerging contaminants in aqueous solutions. Chem. Eng. J. **279**, 788–798 (2015). https://doi.org/10.1016/j.cej.2015.05.104
42. Tran, H.N., You, S.J., Chao, H.P.: Thermodynamic parameters of cadmium adsorption onto orange peel calculated from various methods: A comparison study. J. Environ. Chem. Eng. **4**, 2671–2682 (2016). https://doi.org/10.1016/j.jece.2016.05.009
43. Tran, H.N., You, S.J., Hosseini-Bandegharaei, A., Chao, H.P.: Mistakes and inconsistencies regarding adsorption of contaminants from aqueous solutions: A critical review. Water Res. **120**, 88–116 (2017). https://doi.org/10.1016/j.watres.2017.04.014
44. Trovó, A.G., Nogueira, R.F.P.: Diclofenac abatement using modified solar photo-fenton process with Ammonium Iron(III) citrate. J. Braz. Chem. Soc. **22,** 1033–1039 (2011). https://doi.org/10.1590/S0103-50532011000600005
45. Vergili, I.: Application of nanofiltration for the removal of carbamazepine, diclofenac and ibuprofen from drinking water sources. J. Environ. Manage. **127**, 177–187 (2013). https://doi.org/10.1016/j.jenvman.2013.04.036
46. Vogna, D., Marotta, R., Napolitano, A., Andreozzi, R., D'Ischia, M.: Advanced oxidation of the pharmaceutical drug diclofenac with UV/H 2O2 and ozone. Water Res. **38**, 414–422 (2004). https://doi.org/10.1016/j.watres.2003.09.028
47. Xie, J., Liu, M., He, M., Liu, Y., Li, J., Yu, F., Lv, Y., Lin, C., Ye, X.: Ultra-efficient adsorption of diclofenac sodium on fish-scale biochar functionalized with H3PO4 via synergistic mechanisms. Environ. Pollut. **322**, (2023). https://doi.org/10.1016/j.envpol.2023.121226
48. Yang, H., Chen, P., Chen, W., Li, K., Xia, M., Xiao, H., Chen, X., Chen, Y., Wang, X., Chen, H.: Insight into the formation mechanism of N, P co-doped mesoporous biochar from H3PO4 activation and NH3 modification of biomass. Fuel Process. Technol. **230**, 107215 (2022). https://doi.org/10.1016/j.fuproc.2022.107215

49. Yin, R., Guo, W., Wang, H., Du, J., Wu, Q., Chang, J.S., Ren, N.: Singlet oxygen-dominated peroxydisulfate activation by sludge-derived biochar for sulfamethoxazole degradation through a non-radical oxidation pathway: Performance and mechanism. Chem. Eng. J. **357**, 589–599 (2019). https://doi.org/10.1016/j.cej.2018.09.184
50. Zeng, H., Zeng, H., Zhang, H., Shahab, A., Zhang, K., Lu, Y., Nabi, I., Naseem, F., Ullah, H.: Efficient adsorption of Cr (VI) from aqueous environments by phosphoric acid activated eucalyptus biochar. J. Clean. Prod. **286**, (2021). https://doi.org/10.1016/j.jclepro.2020.124964
51. Zhang, S., Dong, Y., Yang, Z., Yang, W., Wu, J., Dong, C.: Adsorption of pharmaceuticals on chitosan-based magnetic composite particles with core-brush topology. Chem. Eng. J. **304**, 325–334 (2016). https://doi.org/10.1016/j.cej.2016.06.087